



HHS Public Access

Author manuscript

ACS Appl Mater Interfaces. Author manuscript; available in PMC 2018 May 31.

Published in final edited form as:

ACS Appl Mater Interfaces. 2017 May 31; 9(21): 17681–17687. doi:10.1021/acsami.7b04718.

Trimetallic Nitride Endohedral Fullerenes Carboxyl-Gd₃N@C₈₀: A New Theranostic Agent for Combating Oxidative Stress and Resolving Inflammation

Tinghui Li^{‡,†}, Li Xiao^{§,ID,†}, Jiezuang Yang[§], Mengmeng Ding[§], Zhiguo Zhou^{||}, Leslie LaConte[⊥], Li Jin[§], Harry C. Dorn^{‡,⊥,*,ID}, and Xudong Li^{§,*}

[‡]Department of Chemistry, Virginia Polytechnic Institute and State University, Blacksburg, Virginia 24061, United States

[§]Department of Orthopaedic Surgery, University of Virginia, Charlottesville, Virginia 22903, United States

[⊥]Virginia Tech Carilion Research Institute, Roanoke, Virginia 24016, United States

^{||}Luna Innovations Inc. Danville, Virginia 24541, United States

Abstract

Antioxidative and anti-inflammatory effects of trimetallic nitride endohedral fullerenes carboxyl-Gd₃N@C₈₀, a newly developed magnetic resonance imaging (MRI) contrast agent, were investigated. All hydrochalarone and carboxyl-functionalized fullerenes showed effective radical (hydroxyl and superoxide anion) scavenging, whereas the carboxyl-Gd₃N@C₈₀ more efficiently attenuated lipopolysaccharide (LPS) induced oxidative stress in macrophages. Carboxyl-Gd₃N@C₈₀ also suppressed LPS-elicited mRNA expression of pro-inflammatory inducible nitric oxide synthase and tumor necrosis factor- α , and upregulated antioxidative enzyme axis Nrf2 and heme oxygenase-1, possibly via ERK but not AKT signaling pathways. Therefore, carboxyl-Gd₃N@C₈₀ held a great promise in becoming a novel theranostic nanoplatform for simultaneously deliver MRI contrast and therapeutic functions to inflammation-related diseases.

Graphical Abstract

*Corresponding Authors. hdorn@vt.edu. xl2n@virginia.edu.

ORCID 

Li Xiao: 0000-0003-1403-7472

Harry C. Dorn: 0000-0002-3150-5314

[†]T.L. and L.X. contributed equally to the current work.

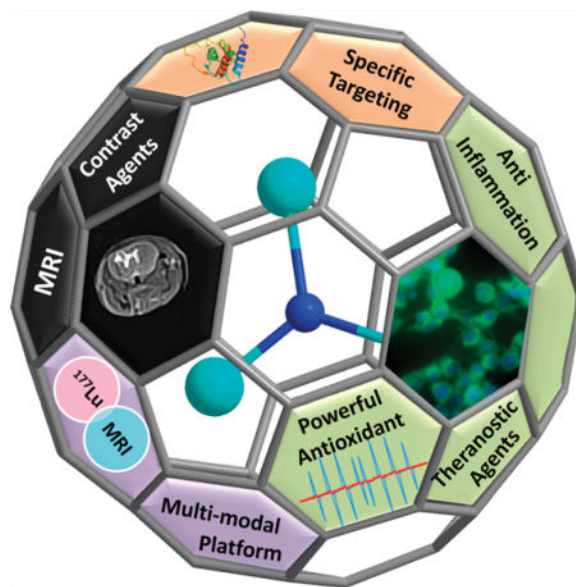
ASSOCIATED CONTENT

Supporting Information

The Supporting Information is available free of charge on the [ACS Publications website](https://pubs.acs.org/doi/10.1021/acsami.7b04718) at DOI: 10.1021/acsami.7b04718.

Chemical material, electron paramagnetic resonance (EPR) spectroscopic measurements, in vitro culture of Raw 264.7 macrophages, nanoparticle screening assay against LPS-induced intracellular reactive oxygen species (ROS), cell viability assay, fluorescence imaging of intracellular ROS, Griess assay, real-time reverse transcription polymerase chain reaction. Immunofluorescence staining of nuclear factor erythroid 2-related factor 2 (Nrf2) and fluorescence image analysis, Western blotting and statistical analysis (PDF)

The authors declare no competing financial interest.



Keywords

trimetallic nitride endohedral fullerenes; theranostic; oxidative stress; inflammation; macrophage; ERK; AKT

Oxidative stress is characterized by increased level of reactive oxygen species (ROS) and/or reactive nitrogen species (RNS). This may be caused by impaired antioxidant enzyme activity, low concentrations of antioxidant, and excessive ROS production. Under the normal physiological condition, ROS play essential roles in maintaining redox signaling balance and controlling cell survival. However, high levels of ROS may induce alteration or damage to DNA, proteins, and lipids, which has been implied in the pathogenesis of a number of diseases,¹⁻³ including cancer, diabetic mellitus, cardiovascular, neurodegeneration, skeletal muscle degeneration, osteoarthritis, and intervertebral disc degeneration. Antioxidative supplements, enzymes, nanoparticles, and inhibitors for ROS-generating nicotinamide adenine dinucleotide phosphate-oxidase (NADPH) oxidases have become potential therapeutic interventions to combat oxidative stress via scavenging/neutralizing ROS directly and/or inhibiting downstream deleterious effects of ROS. Among them, nanoparticles with intrinsic ROS scavenging, and antioxidant properties exhibit superior pharmacological profiles to other antioxidants via enhanced absorption, bioavailability, and readily functionalization for targeted delivery. These nanoparticles include mesoporous silica, cerium oxide, and fullerene.

Fullerene is a molecule of carbon in the form of a hollow sphere with diversified applications, such as photovoltaic and electronic devices, surface coating material, and antioxidant.⁴ Shortly after the discovery of fullerenes in the 1990s, endohedral metallofullerenes (EMF) and trimetallic nitride endohedral fullerenes (TNT-EMF) were recognized for their multifunctional capabilities in biomedical applications. Functionalized gadolinium-loaded fullerenes, Gd@C₈₂ and Gd₃N@C₈₀, attracted much attention as a potential new nanoplatform for next-generation magnetic resonance imaging (MRI) contrast

agents, given their inherent higher ^1H relaxivity than most commercial contrast agents.^{5–13} The fullerene cage is an extraordinarily stable species which makes it extremely unlikely to break and release the toxic Gd metal ions into the bioenvironment. In addition, radiolabeled metals could be encapsulated in this robust carbon cage to deliver therapeutic irradiation.^{14–16} In the past decade, we have endeavored to discover a series of functionalized $\text{Gd}_3\text{N}@C_{80}$ for MRI detection of various pathological conditions, such as chronic osteomyelitis and brain cancer.^{13,17,18}

Fullerene is a powerful antioxidant due to delocalization of the π -electrons over the carbon cage, which can readily react with free radicals and subsequently delivers a cascade of downstream possessions in numerous biomedical applications.⁴ Numerous studies have demonstrated the free radical scavenging capabilities, to such a degree that fullerenes have been described as “free radical sponges”.¹⁹ Functionalized C_{60} and $\text{Gd}@C_{82}$ have been reported to quench radicals efficiently.^{8,12,20} However, the therapeutic potential of functionalized $\text{Gd}_3\text{N}@C_{80}$ has not been investigated. If these TNT-EMF exhibit antioxidative and anti-inflammatory properties, similar as their nonmetal or monometal counterparts, they would hold great promise as a novel class of theranostic agent in combating oxidative stress and resolving inflammation, given their inherent MRI applications.

In the current study, we performed chemical and biological screening on three $\text{Gd}_3\text{N}@C_{80}$ -based derivatives, including $\text{Gd}_3\text{N}@C_{80}(\text{OH})_{30}(\text{CH}_2\text{CH}_2\text{COOH})_{20}$ (carboxyl- $\text{Gd}_3\text{N}@C_{80}$)¹⁷ (Figure 1a) and hydrochalarone-1 (HyC-1- $\text{Gd}_3\text{N}@C_{80}$), hydrochalarone-3 (HyC-3- $\text{Gd}_3\text{N}@C_{80}$), ($\text{Gd}_3\text{N}@C_{80}\text{-Rx}$, where $\text{R} = [\text{N}(\text{OH})(\text{CH}_2\text{CH}_2\text{O})_n\text{CH}_3]_x$, $n = 1, 3, 6$ and $x = 10\text{--}22$)¹⁰ (Figure 1b) to assess their radical scavenging, antioxidative, and anti-inflammatory properties. The related characterization of these three compounds were reported in the earlier papers.^{10,17} We demonstrated intriguing results on structure–activity relationship, and investigated molecular and cellular mechanisms regarding the biological/therapeutic performance of the most promising fullerene carboxyl- $\text{Gd}_3\text{N}@C_{80}$ using an in vitro macrophage model. First of all, we utilized electron paramagnetic resonance (EPR) techniques to evaluate the capability of carboxyl- $\text{Gd}_3\text{N}@C_{80}$ (Figure 1a), HyC-1- $\text{Gd}_3\text{N}@C_{80}$ and HyC-3- $\text{Gd}_3\text{N}@C_{80}$ (Figure 1b) to eliminate ROS in a cell free system, which provided direct evidence in their radical scavenging capabilities. As hydroxyl radical ($\bullet\text{OH}$) and superoxide radical anion ($\text{O}_2^{\bullet-}$), are the most common ROS in the body, they were chosen as model in this experiment. Due to the relatively low sensitivity of EPR detection and short-lived biological free radicals, exogenous spin traps were used. The EPR assay was based on the competition between the trapping agents, and functionalized fullerenes for radicals. Hydroxyl radicals were generated by the classical Fenton reaction, which involves the reaction of FeSO_4 and H_2O_2 . The concentration of H_2O_2 was $200\ \mu\text{M}$, DEPMPO was $500\ \mu\text{M}$, which was 9 times higher than the metallofullerene derivatives ($56\ \mu\text{M}$). The superoxide radical anion was generated by using the xanthine/xanthine oxidase system. The concentration of trapping agent, BMPO, was about 500 times concentrated than metallofullerenes. As shown in Figure 1c, d, a portion of radicals were quenched by the functionalized metallofullerenes, and the residues were captured by the trapping agents to yield adducts of DEPMPO–OH and BMPO–OOH, respectively. After treatment with $\text{Gd}_3\text{N}@C_{80}$ -based nanoparticles, EPR profiles of both DEPMPO–OH and BMPO–OOH

were significantly declined compared with the control. The inhibitory effects of three Gd₃N@C₈₀ derivatives were further summarized in Figure 1e. Although carboxyl-Gd₃N@C₈₀ exhibited the highest scavenging capability toward hydroxyl radicals among all three fullerenes, there was no difference between HyC-1-Gd₃N@C₈₀ and HyC-3-Gd₃N@C₈₀ in hydroxyl radical elimination. These three Gd₃N@C₈₀-based derivatives exhibited similar quenching ability for superoxide radical anions. Such desired but slightly varied radical scavenging properties of these functionalized Gd₃N@C₈₀ could be attributed to their different surface functionalization. After chemical modification, some of the π -system of fullerene framework is altered by replacing a cage carbon with another unit. The active hydroxyl radical could attack the electron-deficient areas on the carbon cage surface or be stabilized by forming hydrogen bonds with the proximate hydroxyl protons of functionalized Gd₃N@C₈₀. There were more hydroxyl groups on the cage of carboxyl-Gd₃N@C₈₀ as compared to HyC-1-Gd₃N@C₈₀ and HyC-3-Gd₃N@C₈₀ (30 vs. 10–22), making the carboxyl-Gd₃N@C₈₀ a more efficient nanoparticle on quenching hydroxyl radicals. Our observation is also consistent with previous reports that modification the fullerene cage with *tris*-malonic acid leads to electron deficient areas on the surface which facilitate binding of superoxide radical anions.²¹ In addition, binding of a second superoxide radical anions to an adjacent electron deficient area might result in the destruction of this type of radicals to produce H₂O₂, and regeneration of the functionalized metallofullerene in a reaction similar to that catalyzed by superoxide dismutase. The number of –C–O– groups on this three Gd₃N@C₈₀-based derivatives were similar (20 vs. 10–22), hence leading to a similar scavenging effect of superoxide radical anions for all three fullerenes.

Although ROS signaling is a complicated, cell- and tissue-specific, physiological and pathophysiological context, restoring ROS hemostasis has been a well-respected therapeutic strategy to combat oxidative stress and a cascade of pro-inflammatory events.²² To confirm our cell-free EPR assays on radical scavenging, an in vitro macrophage cell model (Raw 264.7 cells with or without LPS stimulation) was adopted for biological characterization. First of all, we observed little cytotoxicity of all three nanoparticles at 0.1, 1, and 10 μ M concentration for up to 24 h with or without LPS treatment (Figures S1 S2). Subsequently, a fluorescence assay was developed by incorporating an intracellular ROS sensitive dye 2',7'-dichlorodihydrofluorescein diacetate (H₂DCFDA) in a 96-well plate. A well-known antioxidative enzyme heme oxygenase-1 (HO-1) inducer protoporphyrin IX cobalt chloride (CoPP) was used as a positive control. Briefly, cells were preincubated with various concentration of nanoparticles (0.1, 1, and 10 μ M) for 20 h and treated with or without LPS (100 ng/mL) for additional 4 h. The green fluorescence emitted from intracellular space indicated the abundance of ROS. As shown in Figure 2, LPS dramatically stimulated intracellular ROS production by ~4-fold compared to non-LPS control (**p* < 0.05 vs control). The positive control CoPP pretreated cells showed a significant inhibitory effect on ROS production in Raw 264.7 cells (Figure 2d) via its known effect in promoting antioxidative enzyme HO-1 activity.²³ Carboxyl-Gd₃N@C₈₀ demonstrated a similar inhibitory trend in alleviating LPS-induced ROS (Figure 2a) in a dose-dependent manner. In contrast, the ROS inhibitory effect of hydrochalarone functionalized HyC-1 (Figure 2b) and HyC-3 (Figure 2c) was not as efficient as carboxyl-Gd₃N@C₈₀ even at 10 μ M. This data corroborated with EPR hydroxyl radical scavenging data, which suggested that carboxyl-

Gd₃N@C₈₀ would be an optimal candidate warranting further investigation. Therefore, we chose carboxyl-Gd₃N@C₈₀ for further biological evaluation.

Both inducible nitrite oxide synthase (iNOS) and tumor necrotic factor-alpha (TNF- α) are pro-inflammatory mediators, which are dramatically up-regulated during LPS-induced inflammatory responses in macrophages, therefore downregulation of iNOS and TNF- α have been considered as a therapeutic marker for anti-inflammatory agents. HO-1 is an endogenous antioxidative microsomal enzyme whose upregulation showed a protective role (such as immune-modulation) in combating oxidative stress and resolving inflammation.²⁴ Nrf2 is a basic leucine zipper (bZIP) protein that regulates the expression of antioxidative proteins, such as HO-1.²⁵ To examine the antioxidative and anti-inflammatory effect of carboxyl-Gd₃N@C₈₀, we pretreated Raw 264.7 cells with nanoparticle at 3.5 μ M for 20 h and LPS for another 4 h. Total RNA were isolated, reverse-transcribed to cDNA, and analyzed with real-time PCR. As shown in Figure 3, LPS significantly promoted the mRNA expression of iNOS (** p < 0.01) and TNF- α compared to the control (***) (p < 0.001). Carboxyl-Gd₃N@C₈₀ treatment markedly suppressed the upregulated iNOS and TNF- α mRNA. In contrast to LPS that possesses no impact on the gene expression of HO-1 (p > 0.05 vs. control), carboxyl-Gd₃N@C₈₀ significantly elevated mRNA level of HO-1 (***) (p < 0.0001 vs control; ### p < 0.0001 vs LPS). In addition, Griess assay to assess nitrite (stable end-product of released NO) in cell media at a later time point illustrated carboxyl-Gd₃N@C₈₀ inhibited LPS-elicited nitric oxide release significantly (Figure S3), consistent with iNOS mRNA expression and prior intracellular ROS screening (Figure 2a). Our immunofluorescence staining data of Nrf2 expression in various treatment groups suggested carboxyl-Gd₃N@C₈₀ effectively elevated the global Nrf2 expression in presence or absence of LPS (***) (p < 0.001 vs control, ### p < 0.001 vs LPS) linking its protective function for antioxidative and anti-inflammatory uses (Figure 3d, e). Primer sequences are listed in Table S1.

Mitogen-activated protein kinase MAPK (p38, ERK1/2, JNK) signaling play crucial roles in regulating pro-inflammatory cytokines and mediators such as TNF- α and iNOS during the course of inflammatory response. In particular, activation of ERK1/2 has been reported to stimulate TNF- α transcription and control the transport of TNF- α mRNA from the nucleus to the cytoplasm.²⁶ To further elucidate the molecular and cellular pathways regarding how carboxyl-Gd₃N@C₈₀ regulated oxidative stress and inflammation in macrophages, phosphorylation of ERK, and Akt proteins were studied using Western blotting. As shown in Figure 4, LPS significantly elevated the phosphorylation of both ERK (***) (p < 0.001) and Akt (* p < 0.05) compared to control groups, whereas carboxyl-Gd₃N@C₈₀ (3.5 μ M) markedly reduced phospho-ERK (### p < 0.001) with no significant effect on the change of phospho-Akt (p > 0.05) compared to LPS groups. These results suggested that carboxyl-Gd₃N@C₈₀ protected macrophages from oxidative stress and inflammatory response primarily via downregulating LPS-induced phosphorylation of ERK but not AKT. Since activation of ERK is an early event in ROS signaling of macrophages activation, predominant regulation of this pathway by carboxyl-Gd₃N@C₈₀ would benefit substantial downstream intracellular targets to lessen oxidative stress and resolve inflammation.

To the best of our knowledge, we report the first discovery here that functionalized Gd₃N@C₈₀ possessed robust radical scavenging properties in solution and suppressed LPS-induced ROS in macrophage cell model, which was predominantly correlated to varied surface functionalization of metallofullerene. Carboxyl-Gd₃N@C₈₀ significantly attenuated LPS-induced iNOS and TNF- α mRNA expression, and correspondingly increased expression antioxidative enzyme HO-1 mRNA and its regulatory protein Nrf2. Such antioxidative and anti-inflammatory effects might be regulated via ERK but not Akt signaling pathways. In summary, we prove the concept that trimetallic nitride endohedral fullerenes, especially carboxyl-Gd₃N@C₈₀ hold great promise in becoming a novel class of theranostic agent against the oxidative stress and inflammation, in combination with their inherited MRI applications.

Supplementary Material

Refer to Web version on PubMed Central for supplementary material.

Acknowledgments

We are grateful to financial support in part from National Institute of Health NIAMS R01AR064792, North American Spine Society, and Orthopaedic Trauma Association. We also appreciate The Biomolecular Analysis Facility at University of Virginia for the fluorescence plate reader.

References

1. Liu H, Yang X, Zhang Y, Dighe A, Li X, Cui Q. Fullerol Antagonizes Dexamethasone-induced Oxidative Stress and Adipogenesis While Enhancing Osteogenesis in a Cloned Bone Marrow Mesenchymal Stem Cell. *J. Orthop. Res.* 2012; 30(7):1051–1057. [PubMed: 22570221]
2. Akhtar MJ, Ahamed M, Alhadlaq HA, Alshamsan A. Mechanism of ROS scavenging and Antioxidant Signalling by Redox Metallic and Fullerene Nanomaterials: Potential Implications in ROS Associated Degenerative Disorders. *Biochim. Biophys. Acta, Gen. Subj.* 2017; 1861(4):802–813.
3. Markovic Z, Trajkovic V. Biomedical Potential of the Reactive Oxygen Species Generation and Quenching by Fullerenes (C₆₀). *Biomaterials.* 2008; 29(26):3561–3573. [PubMed: 18534675]
4. Morry J, Ngamcherdtrakul W, Yantasee W. Oxidative stress in cancer and fibrosis: Opportunity for Therapeutic Intervention with Antioxidant Compounds, Enzymes, and Nanoparticles. *Redox Biol.* 2017; 11:240–253. [PubMed: 28012439]
5. Mikawa M, Kato H, Okumura M, Narazaki M, Kanazawa Y, Miwa N, Shinohara H. Paramagnetic Water-soluble Metallofullerenes Having the Highest Relaxivity for MRI Contrast Agents. *Bioconjugate Chem.* 2001; 12(4):510–514.
6. Fatouros PP, Corwin FD, Chen ZJ, Broaddus WC, Tatum JL, Kettenmann B, Ge Z, Gibson HW, Russ JL, Leonard AP, Duchamp JC, Dorn HC. In vitro and in vivo Imaging Studies of a New Endohedral Metallofullerene Nanoparticle. *Radiology.* 2006; 240(3):756–764. [PubMed: 16837672]
7. Shu CY, Corwin FD, Zhang JF, Chen ZJ, Reid JE, Sun MH, Xu W, Sim JH, Wang CR, Fatouros PP, Esker AR, Gibson HW, Dorn HC. Facile Preparation of a New Gadofullerene-Based Magnetic Resonance Imaging Contrast Agent with High H¹ Relaxivity. *Bioconjugate Chem.* 2009; 20(6): 1186–1193.
8. Yin JJ, Lao F, Fu PP, Wamer WG, Zhao Y, Wang PC, Qiu Y, Sun B, Xing G, Dong J, Liang XJ, Chen C. The scavenging of Reactive Oxygen Species and The Potential for Cell Protection by Functionalized Fullerene Materials. *Biomaterials.* 2009; 30(4):611–21. [PubMed: 18986699]
9. Zhang JF, Fatouros PP, Shu CY, Reid J, Owens LS, Cai T, Gibson HW, Long GL, Corwin FD, Chen ZJ, Dorn HC. High Relaxivity Trimetallic Nitride (Gd₃N) Metallofullerene MRI Contrast Agents with Optimized Functionality. *Bioconjugate Chem.* 2010; 21(4):610–615.

10. Adisheshaiah P, Dellinger A, MacFarland D, Stern S, Dobrovolskaia M, Ileva L, Patri AK, Bernardo M, Brooks DB, Zhou ZG, McNeil S, Kepley C. A Novel Gadolinium-Based Trimetasphere Metallofullerene for Application as a Magnetic Resonance Imaging Contrast Agent. *Invest. Radiol.* 2013; 48(11):745–754. [PubMed: 23748228]
11. Zhang JY, Ye YQ, Chen Y, Pregot C, Li TH, Balasubramaniam S, Hobart DB, Zhang YF, Wi S, Davis RM, Madsen LA, Morris JR, LaConte SM, Yee GT, Dorn HC. Gd₃N@C₈₄(OH)_x: A New Egg-Shaped Metallofullerene Magnetic Resonance Imaging Contrast Agent. *J. Am. Chem. Soc.* 2014; 136(6):2630–2636. [PubMed: 24432974]
12. Li J, Guan M, Wang T, Zhen M, Zhao F, Shu C, Wang C. Gd@C₈₂-(ethylenediamine)₈ Nanoparticle: A New High-Efficiency Water-Soluble ROS Scavenger. *ACS Appl. Mater. Interfaces.* 2016; 8(39):25770–25776. [PubMed: 27610478]
13. Li TH, Murphy S, Kiselev B, Bakshi KS, Zhang JY, Eltahir A, Zhang YF, Chen Y, Zhu J, Davis RM, Madsen LA, Morris JR, Karolyi DR, LaConte SM, Sheng Z, Dorn HC. A New Interleukin-13 Amino-Coated Gadolinium Metallofullerene Nanoparticle for Targeted MRI Detection of Glioblastoma Tumor Cells. *J. Am. Chem. Soc.* 2015; 137(24):7881–7888. [PubMed: 26022213]
14. Shultz MD, Duchamp JC, Wilson JD, Shu CY, Ge JC, Zhang JY, Gibson HW, Fillmore HL, Hirsch JJ, Dorn HC, Fatouros PP. Encapsulation of a Radiolabeled Cluster Inside a Fullerene Cage, ¹⁷⁷Lu_xLu_(3-x)N@C₈₀: An Interleukin-13-Conjugated Radiolabeled Metallofullerene Platform. *J. Am. Chem. Soc.* 2010; 132(14):4980–4981. [PubMed: 20307100]
15. Wilson JD, Broaddus WC, Dorn HC, Fatouros PP, Chalfant CE, Shultz MD. Metallofullerene-Nanoparticle-Delivered Interstitial Brachytherapy Improved Survival in a Murine Model of Glioblastoma Multiforme. *Bioconjugate Chem.* 2012; 23(9):1873–1880.
16. Horiguchi Y, Kudo S, Nagasaki Y. Gd@C₈₂ Metallofullerenes for Neutron Capture Therapy- Fullerene Solubilization by Poly-(ethylene glycol)-block-poly(2-(N, N-diethylamino)ethyl methacrylate) and Resultant Efficacy in vitro. *Sci. Technol. Adv. Mater.* 2011; 12(4):044607. [PubMed: 27877415]
17. Xiao L, Li T, Ding M, Yang J, Rodriguez-Corrales J, LaConte SM, Nacey N, Weiss DB, Jin L, Dorn HC, Li X. Detecting Chronic Post-Traumatic Osteomyelitis of Mouse Tibia via an IL-13Rα2 Targeted Metallofullerene Magnetic Resonance Imaging Probe. *Bioconjugate Chem.* 2017; 28(2):649–658.
18. Shultz MD, Wilson JD, Fuller CE, Zhang JY, Dorn HC, Fatouros PP. Metallofullerene-based Nanoparticle Platform for Brain Tumor Brachytherapy and Longitudinal Imaging in a Murine Orthotopic Xenograft Model. *Radiology.* 2011; 261(1):136–143. [PubMed: 21813738]
19. Li T, Dorn HC. Biomedical Applications of Metal-Encapsulated Fullerene Nanoparticles. *Small.* 2017; 13(8):1603152.
20. Wang J, Chen C, Li B, Yu H, Zhao Y, Sun J, Li Y, Xing G, Yuan H, Tang J, Chen Z, Meng H, Gao Y, Ye C, Chai Z, Zhu C, Ma B, Fang X, Wan L. Antioxidative Function and Biodistribution of [Gd@C₈₂(OH)₂₂]_n Nanoparticles in Tumor-bearing Mice. *Biochem. Pharmacol.* 2006; 71(6):872–881. [PubMed: 16436273]
21. Ali SS, Hardt JJ, Quick KL, Kim-Han JS, Erlanger BF, Huang TT, Epstein CJ, Dugan LL. A Biologically Effective Fullerene (C₆₀) Derivative with Superoxide Dismutase Mimetic Properties. *Free Radical Biol. Med.* 2004; 37(8):1191–202. [PubMed: 15451059]
22. Xu J, Chen L, Li L. Pannexin Hemichannels: A Novel Promising Therapy Target for Oxidative Stress Related Diseases. *J. Cell. Physiol.* 2017; doi: 10.1002/jcp.25906
23. Cai C, Teng L, Vu D, He J-Q, Guo Y, Li Q, Tang X-L, Rokosh G, Bhatnagar A, Bolli R. The Heme Oxygenase 1 Inducer (CoPP) Protects Human Cardiac Stem Cells against Apoptosis through Activation of the Extracellular Signal-regulated Kinase (ERK)/NRF2 Signaling Pathway and Cytokine Release. *J. Biol. Chem.* 2012; 287(40):33720–33732. [PubMed: 22879597]
24. Maamoun H, Zachariah M, McVey JH, Green FR, Agouni A. Heme Oxygenase (HO)-1 Induction Prevents Endoplasmic Reticulum Stress-mediated Endothelial Cell Death and Impaired Angiogenic Capacity. *Biochem. Pharmacol.* 2017; 127:46–59. [PubMed: 28012960]
25. Montana G, Lampiasi N. Substance P Induces HO-1 Expression in RAW 264.7 Cells Promoting Switch towards M2-Like Macrophages. *PLoS One.* 2016; 11(12):e0167420. [PubMed: 27907187]

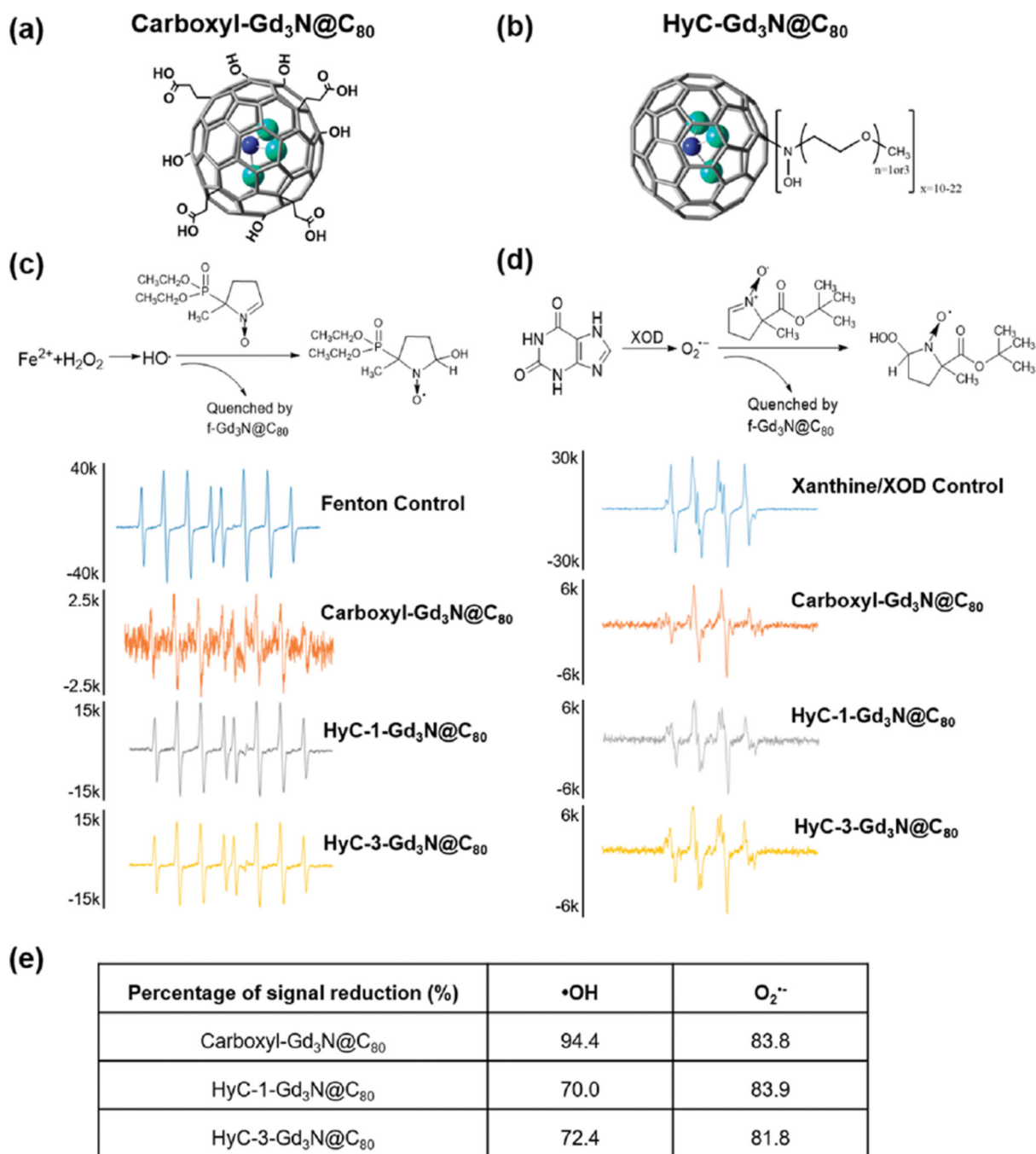
26. Xagorari A, Roussos C, Papapetropoulos A. Inhibition of LPS-stimulated Pathways in Macrophages by the Flavonoid Luteolin. *Br. J. Pharmacol.* 2002; 136(7):1058–1064. [PubMed: 12145106]

Author Manuscript

Author Manuscript

Author Manuscript

Author Manuscript

**Figure 1.**

Radical scavenging properties of three trimetallic nitride endohedral fullerenes. Structures of (a) carboxyl-Gd₃N@C₈₀, (b) HyC-1-Gd₃N@C₈₀ and HyC-3-Gd₃N@C₈₀. (c) Mechanism of the hydroxyl radical production by Fenton reaction and capture by DEPMPO. EPR spectra of the hydroxyl radicals captured by DEPMPO with and without Gd₃N@C₈₀ derivatives. Ultrapure water was used as a control. (d) Mechanism of superoxide radical production by xanthine/xanthine oxidase (XOD) system and capture by BMPO. EPR spectra of superoxide radicals captured by BMPO with and without Gd₃N@C₈₀ derivatives. PBS was used as a

control. (e) Table summary of scavenging capabilities of hydroxyl radical and superoxide radical anion by three Gd₃N@C₈₀ derivatives, carboxyl-Gd₃N@C₈₀, HyC-1-Gd₃N@C₈₀, and HyC-3-Gd₃N@C₈₀.

Author Manuscript

Author Manuscript

Author Manuscript

Author Manuscript

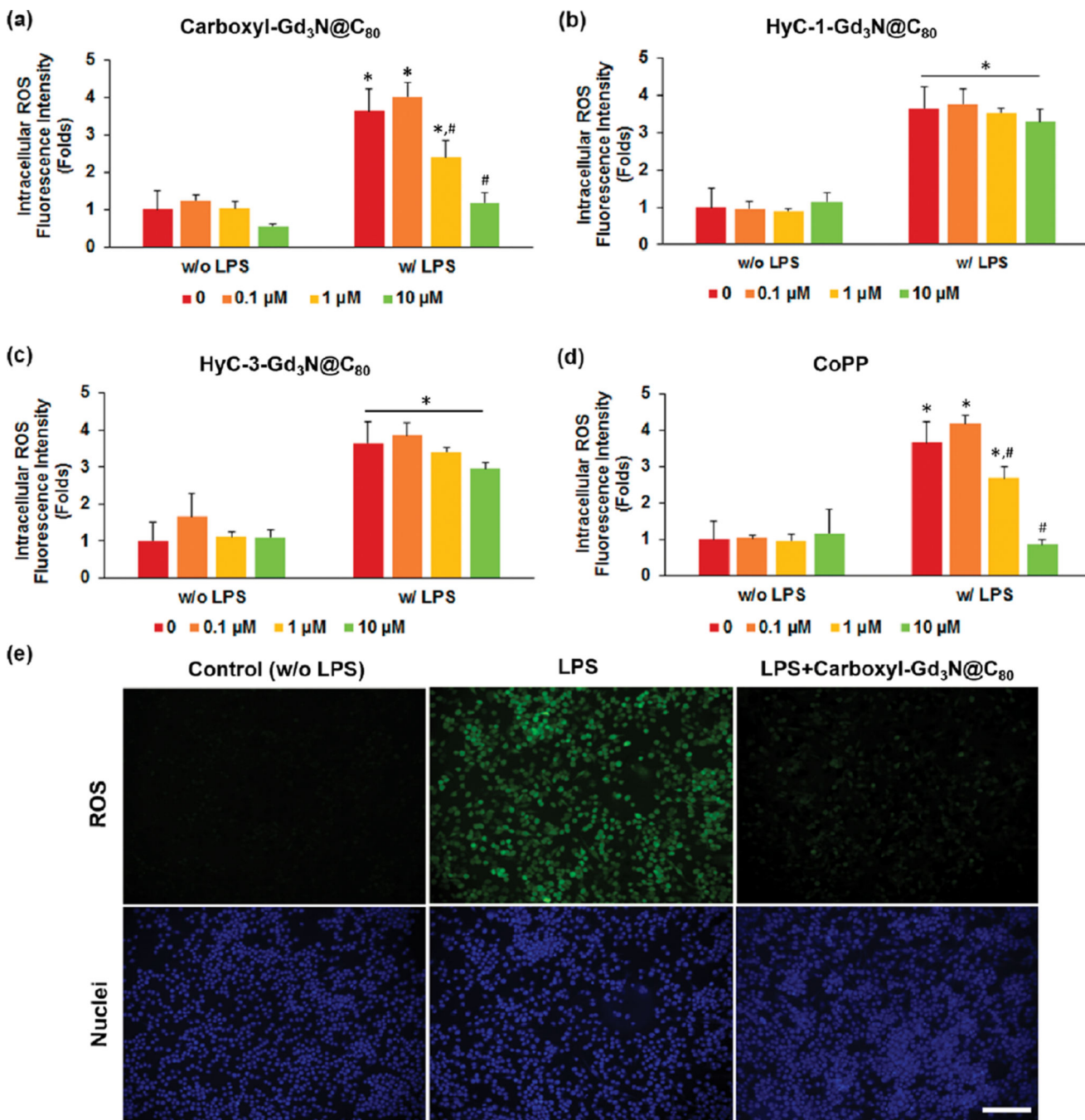


Figure 2. Biological screening of trimetallic nitride endohedral fullerenes for quenching LPS-induced reactive oxygen species (ROS). Raw 264.7 cells were treated with nanoparticles at various concentration (0, 0.1, 1, and 10 μ M) in serum-free medium for 20 h, stimulated with or without LPS (100 ng/mL) for another 4 h, followed by intracellular ROS staining with 5 μ M 2',7' dichlorodihydrofluorescein diacetate (H₂DCFDA) and fluorescence plate reading at E_x/E_m of 495/525 nm. (a) Carboxyl-Gd₃N@C₈₀ exhibited dose-dependent efficacy in attenuating LPS-induced excessive ROS, in a similar fashion as (d) the positive control

protoporphyrin IX cobalt chloride (CoPP), a well-known heme oxygenase-1 inducer. In contrast, (b) HyC-1 and (c) HyC-3 showed no or little reduction in LPS-elicited ROS generation. (e) Representative fluorescence images of intracellular ROS illustrated robust ROS-scavenging activity of carboxyl-Gd₃NC80. Image taken at ×200 magnification. Scale bar represented 100 μm. **p* < 0.05 vs non-LPS control, #*p* < 0.05 vs LPS-treated groups.

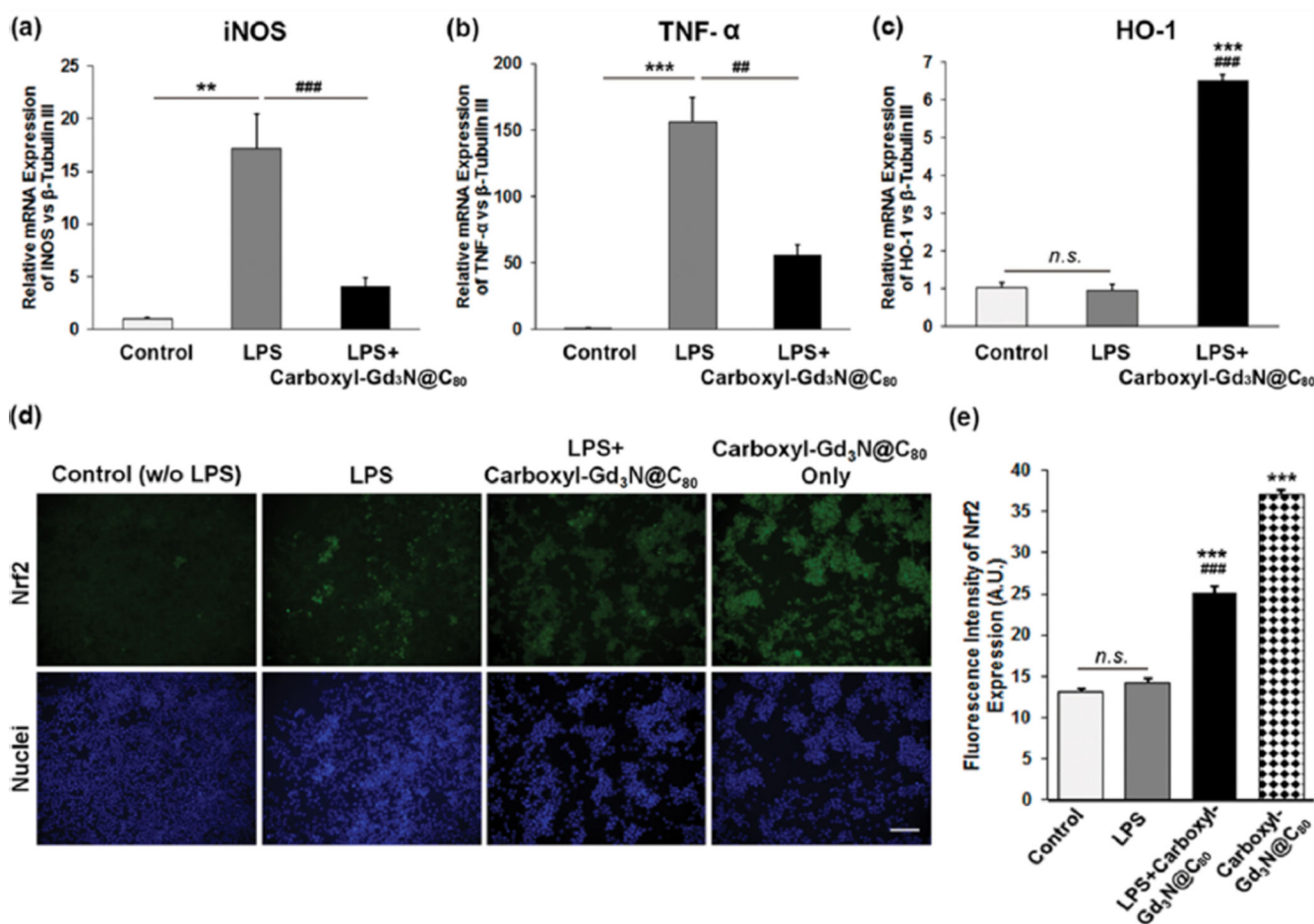


Figure 3. Carboxyl-Gd₃N@C₈₀ protected Raw 264.7 cells from LPS-induced oxidative stress and upregulated pro-inflammatory cytokine via elevating Nrf2 expression. Cells were pretreated with carboxyl-Gd₃N@C₈₀ (3.5 μM) for 20 h before treatment of LPS (100 ng/mL) for 4 h. (a) Real-time reverse transcription polymerase chain reaction (RT-PCR) suggested LPS stimulation significantly increased mRNA expression of inducible nitric oxide synthase (iNOS) (***p* < 0.01 vs control), whereas carboxyl-Gd₃N@C₈₀ dramatically reversed such induction (###*p* < 0.001 vs LPS). (b) Similarly, the upregulation of pro-inflammatory cytokine tumor necrosis factor-α (TNF-α) (****p* < 0.001 vs control) upon LPS treatment was significantly alleviated by carboxyl-Gd₃N@C₈₀ (##*p* < 0.01 vs LPS). (c) The antioxidative enzyme heme oxygenase-1 (HO-1) was significantly enhanced by carboxyl-Gd₃N@C₈₀ (****p* < 0.001 vs control, ###*p* < 0.001 vs LPS) but it was not altered by LPS stimulation. (d) Immunofluorescence staining of Nrf2, a key antioxidative enzyme regulator, was dramatically increased upon nanoparticle treatment in the present and absence of LPS, whereas no significant intensity difference was observed in LPS-treated cells. (e) Mean fluorescence intensity analysis of d suggested carboxyl-Gd₃N@C₈₀ effectively upregulated the protective Nrf2 protein expression (****p* < 0.001 vs control, ###*p* < 0.001 vs LPS). Experiments were repeated three times (*n* = 3). Scale bar in d represented 100 μm.

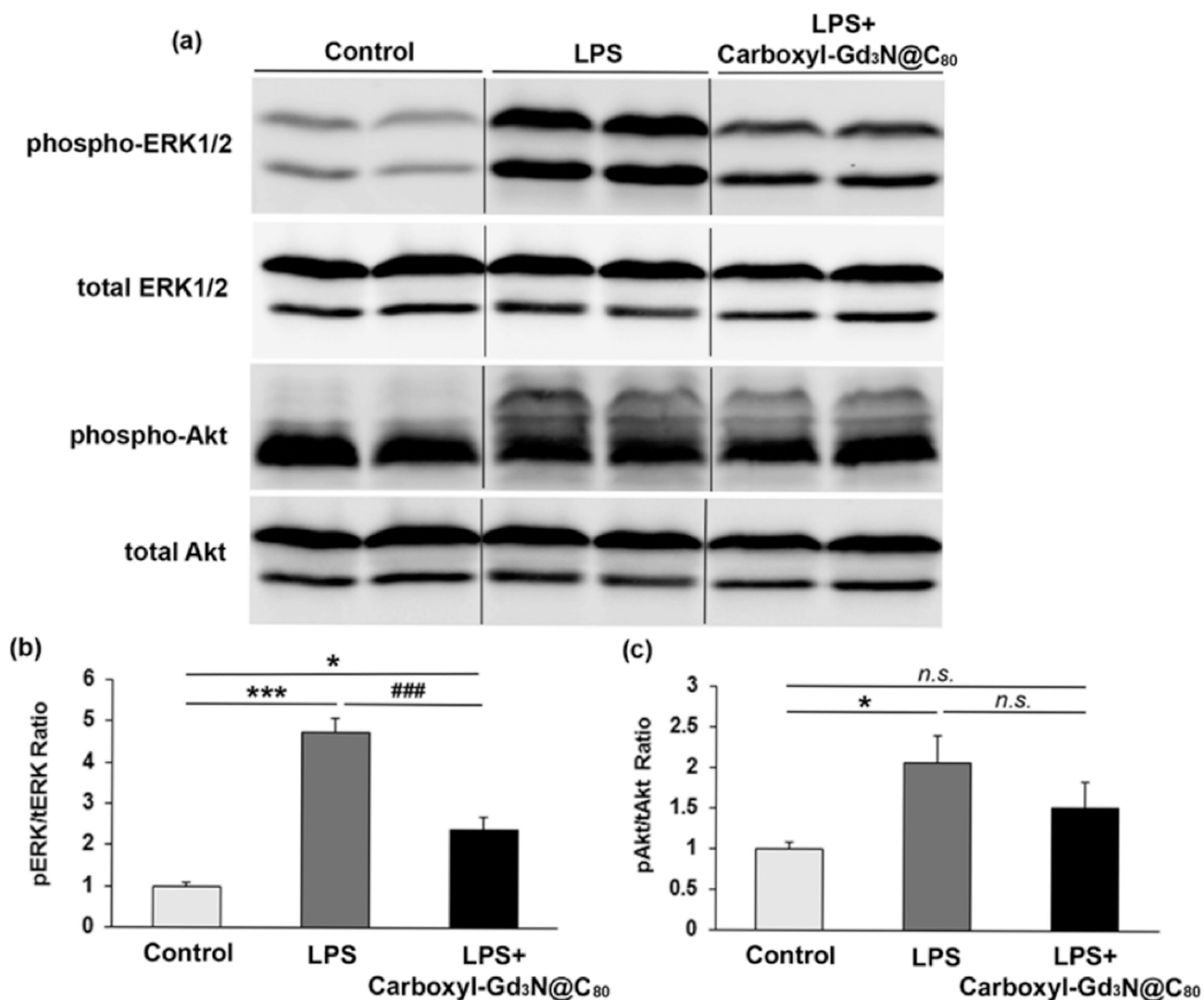


Figure 4. Carboxyl-Gd₃N@C₈₀ rescued Raw 264.7 cells from LPS-induced oxidative stress via ERK and Akt pathways. (a) Representative immunoblotting analysis of phospho-ERK, total ERK, phospho-Akt, and total Akt of cell lysates subjected to different treatments. Cells were preincubated with carboxyl-Gd₃N@C₈₀ (3.5 μ M) for 20 h and treated with or without LPS (100 ng/mL) for another 4 h. (b) Quantification of pERK/tERK ($n = 4$) intensity showed carboxyl-Gd₃N@C₈₀ significantly reversed LPS-induced ERK phosphorylation. (c) Quantitation analysis of pAkt/tAkt ($n = 4$) exhibited some increase in p-Akt upon LPS stimulation, which was not significantly reduced by carboxyl-Gd₃N@C₈₀ pretreatment. Note, * $p < 0.05$, *** $p < 0.001$ vs control; ### $p < 0.001$ vs LPS group.